Cortical and subcortical grey matter micro-structure is associated with polygenic risk for schizophrenia

Eva-Maria Stauffer[1,*], Richard A.I. Bethlehem[1,†], Varun Warrier[1,†], Graham K. Murray[1,2,3], Rafael Romero-Garcia[1], Jakob Seidlitz[4,5], and Edward T. Bullmore[1]

[1]University of Cambridge, Department of Psychiatry, Cambridge Biomedical Campus, CB2 0SZ, UK
[2]Cambridgeshire and Peterborough NHS Trust, Elizabeth House, Fulbourn Hospital, Cambridge CB21 5EE, UK
[3]Institute for Molecular Bioscience, University of Queensland, St Lucia 4072, Australia
[4]Department of Child and Adolescent Psychiatry and Behavioral Science, Children's Hospital of Philadelphia, Philadelphia, PA, USA
[5]Department of Psychiatry, University of Pennsylvania, Philadelphia, PA, USA
[*]corresponding author(s): Eva-Maria Stauffer (ems206@cam.ac.uk)
[†]these authors contributed equally to this work

ABSTRACT

Background
Recent discovery of hundreds of common gene variants associated with schizophrenia has enabled polygenic risk scores (PRS) to be measured in the population. It is hypothesized that normal variation in genetic risk of schizophrenia should be associated with MRI changes in brain morphometry and tissue composition.

Methods
We used the largest extant genome-wide association dataset (N = 69,369 cases and N = 236,642 healthy controls) to measure PRS for schizophrenia in a large sample of adults from the UK Biobank (Nmax = 29,878) who had multiple micro- and macro-structural MRI metrics measured at each of 180 cortical areas and seven subcortical structures. Linear mixed effect models were used to investigate associations between schizophrenia PRS and brain structure at global and regional scales, controlled for multiple comparisons.

Results
Micro-structural phenotypes were more robustly associated with schizophrenia PRS than macro-structural phenotypes. Polygenic risk was significantly associated with reduced neurite density index (NDI) at global brain scale, at 149 cortical regions, and five subcortical structures. Other micro-structural parameters, e.g., fractional anisotropy, that were correlated with NDI were also significantly associated with schizophrenia PRS. Genetic effects on multiple MRI phenotypes were co-located in temporal, cingulate and prefrontal cortical areas, insula, and hippocampus.

Conclusions
We show widespread cortical and subcortical grey matter micro-structure associations with schizophrenia PRS. Across all investigated phenotypes NDI, a measure of the density of myelinated axons and dendrites, showed the most robust associations with schizophrenia PRS. We interpret these results as indicative of reduced density of myelinated axons and dendritic arborization in large-scale cortico-subcortical networks mediating the genetic risk for schizophrenia.

Keywords
NODDI, DWI, false discovery rate, PheWAS, UK Biobank, polygenic risk

Introduction

Schizophrenia is a major mental health disorder with a lifetime prevalence of 1% characterised by hallucinations, delusions, blunted affect, and deficits in planning and communication [1]. Its pathogenesis is substantially genetic [2] with twin and familial heritability estimates of approximately 80% [3, 4], and SNP heritability of approximately 24% [5]. The most recent genome-wide association study (GWAS) identified 270 risk-associated loci, enriched for genes with high expression in the brain and neuronal processes [5]. These and other GWAS data allow the construction of polygenic risk scores (PRS), that explain up to 7.7 % of the variance in schizophrenia in European samples [5]. PRS are normally distributed in the general population, indexing the common genetic liability for schizophrenia, and can be used to investigate the shared genetics between schizophrenia, neurodevelopmental trajectories and brain morphology [6].

The genetic liability for schizophrenia is thought to cause proximal changes in brain structure and function, which then result in distal changes in psychological function and clinical symptoms characteristic of schizophrenia [7, 8, 9, 10]. Although cortical and subcortical brain structural abnormalities have been consistently reported in schizophrenia case-control studies [11, 12], and are substantially heritable [13, 14], the current evidence linking MRI markers of brain structure to polygenic risk for schizophrenia is inconsistent [15]. Recent large-scale studies reported no significant associations between PRS and volume of subcortical nuclei [16, 17, 18]. Some studies have reported significant negative associations between PRS and global brain measures, such as total white matter volume (WMV) [19] or mean cortical thickness (CT) [20]; but effect sizes have been small (mean CT β = -.043, R2 = 0.2 %) and not consistently significant between studies [15, 16]. Cortical thickness of insular cortex was specifically associated with polygenic risk for schizophrenia (β= .05, R2 = 0.2%) [20] but most prior studies have not found significant associations between PRS and regional cortical brain anatomy [15].

The current lack of clear evidence for an effect of genetic risk for schizophrenia on brain MRI phenotypes could be attributable to the relatively small sample sizes of prior genetic neuroimaging studies ($100 < N < 15,000$), which were likely under-powered to detect small polygenic effects [15, 18, 20]. Inherently low power to refute the null hypothesis when it is false is necessarily exacerbated when the probability of type 1 error is appropriately adjusted to control for multiple testing at hundreds of cortical and subcortical regions [20]. However, in addition to these statistical explanations for failure to detect PRS association with MRI phenotypes, it is possible that there is also a more biological explanation. The MRI phenotypes so far investigated have mostly been macro-structural measures of brain morphometry, e.g., cortical thickness, which are relatively coarse-grained compared to the predicted effects of PRS on tissue composition and cellular organization.

Case-control studies of schizophrenia have replicably reported significant reductions in regional cortical thickness (CT), surface area (SA) [11], grey matter volume (GMV) [21], intrinsic curvature (IC) [22] and local gyrification index (LGI) [23]. These are all macro-structural markers of brain morphology that are measured on the basis of all voxels representing each cortical or subcortical region (O $\sim$ cm^3). Micro-structural MRI phenotypes, in contrast, are measured at each voxel (O $\sim$ mm^3) and thus provide finer-grained information about the cellular composition of grey matter tissue. Case-control studies of schizophrenia have increasingly reported significant differences in micro-structural phenotypes [24], such as increased mean diffusivity (MD) in frontal, temporal, insular and visual cortex [25, 26, 27], decreased fractional anisotropy (FA) in the enthorinal cortex [28], decreased neurite density index (NDI) in temporal pole, hippocampus and parahippocampal gyrus [24], and reduced orientation dispersion index (ODI) in the prefrontal cortex [29].

On this basis, we hypothesized that macro- and micro-structural MRI markers of abnormal grey matter tissue composition should be associated with polygenic risk for schizophrenia. We analysed multimodal MRI and genotype data from N $\sim$ 30,000 participants from the UK Biobank to conduct a comprehensive phenome-wide association study with nine brain MRI phenotypes (**Fig.1**). In 180 bilateral cortical areas we measured five macro-structural metrics (CT, SA, GMV, LGI and IC) and four micro-structural metrics of brain morphology (FA, MD, NDI and ODI); and analogous measures for seven subcortical structures where applicable (e.g. GMV, FA, MD, NDI and ODI). We used the largest available GWAS dataset for schizophrenia ($N = 69,369$ cases and $N = 236,642$ controls) to construct schizophrenia PRS for each subject [5]. We expected that this combination of increased sample sizes for PRS estimation, and multi-parameter MRI measurement, of both macro- and micro-structural metrics, would enhance statistical power to test the hypothesis that macro- and micro-structural MRI phenotypes are associated with polygenic risk for schizophrenia in the population.

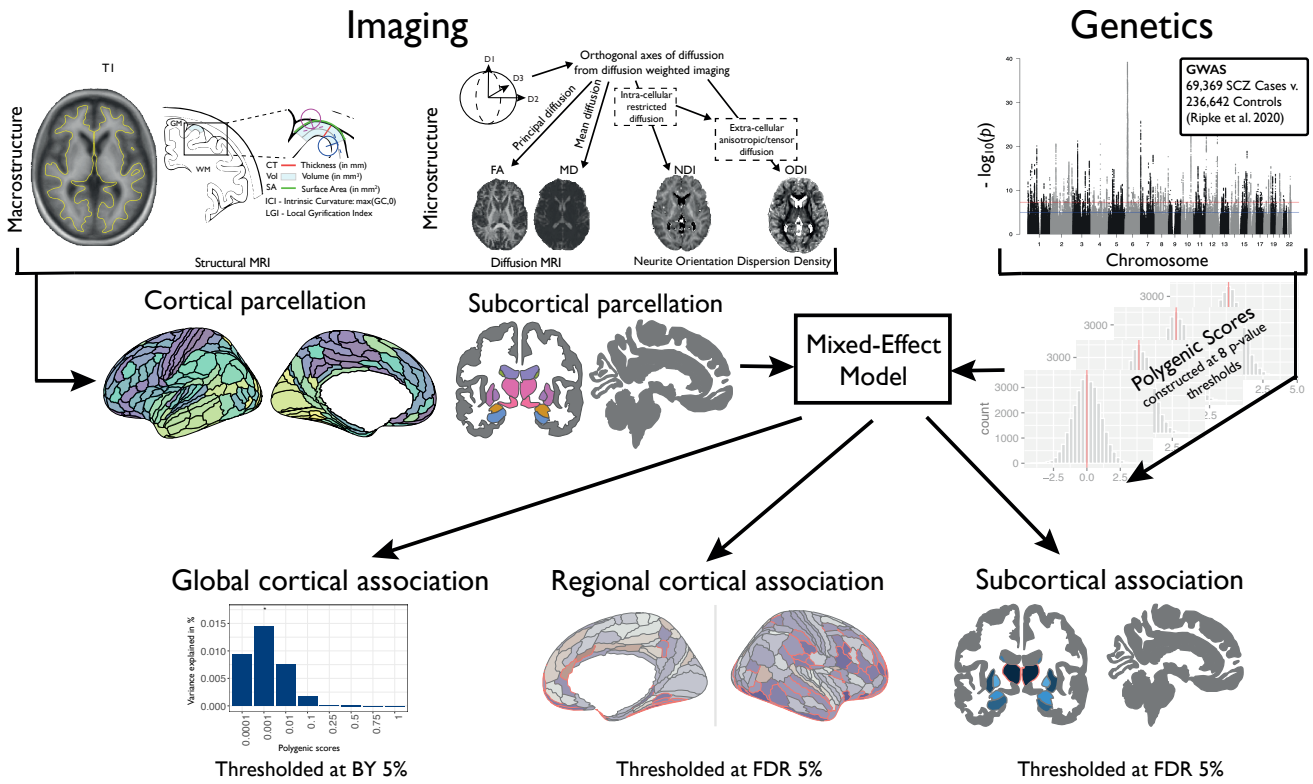

Figure 1. Schematic summary of the study. We estimated five macro-structural metrics and four micro-structural metrics at each of 180 bilateral cortical areas, and on average over all cortical areas, for variable numbers of subjects in the UK Biobank for whom quality-controlled data were available: for cortical thickness (CT), $N = 29,778$; surface area (SA), $N = 29,777$; grey matter volume (GMV), $N = 29,778$; intrinsic curvature (IC), $N = 29,676$; local gyrification index (LGI), $N = 27,086$; fractional anisotropy (FA), $N = 28,232$; mean diffusivity (MD), $N = 28,165$; neurite density index (NDI), $N = 27,632$; and orientation dispersion index (ODI), $N = 27,658$. We also estimated one macro-structural metric and four micro-structural metrics at each of seven subcortical regions (amygdala, accumbens, caudate, putamen, pallidum, hippocampus, and thalamus): GMV, $N = 29,854 - 29,878$; FA, $N = 28,192 - 28,238$; MD, $N = 27,664 - 28,154$; NDI, $N = 27,590 - 27,638$; and ODI, $N = 27,600 - 27,658$. Polygenic risk scores for schizophrenia (PRS) were based on GWAS data from 69,396 cases and 236,642 controls and were calculated for each participant at eight P_{SNP}-value thresholds for inclusion of significant variants, using the clumping and thresholding approach [30].To assess associations between multiple schizophrenia polygenic risk scores and cortical phenotypes, we first used mixed effect models to identify which P_{SNP}-value threshold(s) produced the PRS most strongly associated with each cortical metric at global scale (Benjamini-Yekutieli corrected 5%). We then used mixed effect models to test the association between the globally most predictive PRS for each metric at each cortical area, controlling for multiple comparisons with the false discovery rate (FDR) at 5%. For subcortical structures, we tested for association between each MRI metric and each of eight polygenic risk scores, with FDR = 5%.

Methods and Materials

Participants

The data was provided by the UK Biobank, a population-based cohort of >500,000 subjects aged between 39 and 73 years, who provided informed consent for assessment at one of 22 UK centres [31]. We focused on a subset of N = 40,680 UK Biobank participants for whom individual genotype and multimodal MRI data, were available for download (February 2020); **Fig.S2**. We excluded participants with incomplete MRI data, or with a diagnosis of schizophrenia (self-reported or by ICD-10 clinical diagnosis; see **SI Methods**). Prior to analysis of each MRI phenotype, we additionally excluded participants who were robustly defined as outliers by global or regional (cortical or subcortical) metrics more than 5 times the median of absolute deviations from the sample median ($\pm$ 5 MAD).

Imaging acquisition and preprocessing

MRI data acquisition for UK Biobank has been described in detail elsewhere [32]. Minimally processed T1 and T2-FLAIR weighted data were downloaded from UK Biobank (application 20904)[1] and further processed with Freesurfer (v6.0.1) [33] using the T2-FLAIR weighted image to improve pial surface reconstruction (**SI Methods**). Reconstruction included bias field correction, registration to stereotaxic space, intensity normalization, skull-stripping, and white matter segmentation. Following reconstruction, the Human Connectome Project (HCP) parcellation [34] was aligned to each individual image and regional metrics were estimated for 180 cortical areas. Minimally processed diffusion-weighted imaging (DWI) data were also obtained from UK Biobank (**SI Methods**) and co-registered with the T1 aligned parcellation template to estimate FA and MD at each region. Additionally, neurite orientation dispersion and density imaging (NODDI) reconstruction was performed using the AMICO pipeline [35]. Documentation and code for these processing pipelines is available on Github [2].

Genotyping and genetic quality control

Genome-wide genotype data was available for N = 488,377 participants. DNA acquisition, imputation and quality control pipelines are described in detail elsewhere [36]. We excluded subjects who were not of primarily European ancestry based on genetic ethnic grouping, as well as subjects with excessive genetic heterozygosity, genotyping rate $\leq$ 95%, mismatch between reported and genetic sex, and individuals with genetic relatedness identified using a genetic relatedness matrix (relatedness $>$ 0.25) [37]. We also excluded single nucleotide polymorphisms (SNPs) with minor allele frequency $\leq$ 0.01, Hardy-Weinberg equilibrium (p $\leq 1 \times 10^{-6}$), variant call rate ($\leq$ 98 %) and an imputation quality score $\leq$ 0.4 resulting in N = 5,366,036 SNPs.

Polygenic risk scores

An individual PRS is calculated by multiplying the number of risk alleles a person carries by the size of each allele's effect and summing the products over all SNPs [38]. We used the computationally efficient P-value clumping and thresholding method in PRSice 2 [5, 30, 38, 39]. First, SNPs were clumped so that only the most strongly associated SNP in a region was retained (r^2 = 0.1, physical distance = 250 kb). Second, probabilistic thresholding was used to construct multiple polygenic scores based on SNPs with varying P_{SNP}-value inclusion thresholds to balance signal to noise ratio [40].

We estimated PRS for N = 29,879 participants with quality controlled genetic and imaging data, using effect sizes for each allele from a large prior GWAS of 7,585,078 SNPs in N = 69,369 schizophrenia cases and N = 236,642 healthy controls [5]. We constructed eight polygenic scores with varying P_{SNP}-value thresholds ($P_{SNP} \leq 0.0001$, ≤ 0.001, ≤ 0.01, ≤ 0.1, ≤ 0.25, ≤ 0.5, ≤ 0.75, ≤ 1) for each individual [20, 41]. PRS's were normally distributed at all P_{SNP}-value thresholds (**SI Methods**) and the number of SNPs included in the calculation at each probability threshold is reported in **Table S1**.

Statistical analysis

Statistical analyses were conducted in R [42]. We performed linear mixed effect models (lme) to investigate the associations between the scaled PRS and each of the scaled MRI phenotypes with covariates including age, age^2, sex, genotype batch, 15 PCs (Data-Field 22006), and x, y and z coordinates of head position in the scanner to control for static-field heterogeneity (Data-Field 25756-25758) [43]. Hemisphere was fitted as a random effect, resulting in 180 regions of interest [16, 20, 44], after testing for PRS-by-hemisphere interactions had demonstrated that none were significant at FDR = 5% (**Tables S2/S3**).

Imaging Phenotype $\sim$ Age + Age2 + Sex + Genotype Batch + 15 genetic principal components + x-coordinate + y-coordinate + z-coordinate + PRS, random = $\sim$1|Hemisphere

First, we modeled the effects of all eight PRS's on each cortical measure at a global scale and identified the most predictive probability threshold for each measure: CT $P_{SNP} \leq 1$, Vol $P_{SNP} \leq 0.1$, SA $P_{SNP} \leq 0.25$, IC $P_{SNP} \leq 0.0001$, LGI $P_{SNP} \leq 0.001$, FA $P_{SNP} \leq 0.001$, MD $P_{SNP} \leq 0.01$, NDI $P_{SNP} \leq 0.001$, ODI $P_{SNP} \leq 0.0001$. Tests for significant association of eight PRS's with nine global cortical MRI metrics results were corrected using the Benjamini-Yekutieli procedure to control FDR at 5%

[1] https://biobank.ctsu.ox.ac.uk/crystal/crystal/docs/brainmri.pdf
[2] https://github.com/ucam-department-of-psychiatry/UKB

over 72 tests [45]. Second, we modeled the effect of the PRS constructed at the P_{SNP}-value most predictive of global variance in each metric on the same metric at each of 180 cortical regions. For linear mixed effect models at regional scale, we additionally included intracranial volume as a covariate to account for head size, and used the Benjamini-Hochberg procedure to control FDR at 5% over 180 cortical regions. For seven subcortical regions, we used the same model to estimate the effect of eight PRS's, constructed at different P_{SNP}-values, on each MRI metric, controlling the FDR at 5% over 56 tests entailed for each metric.

Results

Sample

After quality controls, the final sample for analysis of all cortical areas ranged between $N = 27,086$ and $N = 29,778$, depending on the MRI phenotype; and the sample for subcortical analyses ranged between $N = 27,590$ and $N = 29,878$ depending on the phenotype and the subcortical structure (see **Fig.1** legend). All samples comprised approximately 55% female, 45% male participants aged 40-70 years, with mean age $\sim$ 55 years; see **Tables S4-5** for details.

Global cortical MRI phenotypes

After correction for multiple testing (FDR = 5%), two global metrics were significantly associated with PRS at one or more P_{SNP}-value thresholds. Both were micro-structural phenotypes derived from DWI or NODDI: FA was significantly negatively associated with the PRS constructed with $P_{SNP} \leq 0.001$ and NDI was significantly negatively associated with PRS constructed at P_{SNP}'s ≤ 0.0001, 0.001 and 0.01 (**Fig.2 A, Table S6**). These results imply that subjects with a higher polygenic risk for schizophrenia have decreased global fractional anisotropy and neurite density index "on average" over the whole cortex. The association between the PRS and NDI was more robust to the choice of probability threshold used to construct the risk score; and PRS generally accounted for a larger proportion of the variance in NDI ($\sim$ 0.05 %), compared to FA ($\sim$ 0.02 %) and other metrics investigated.

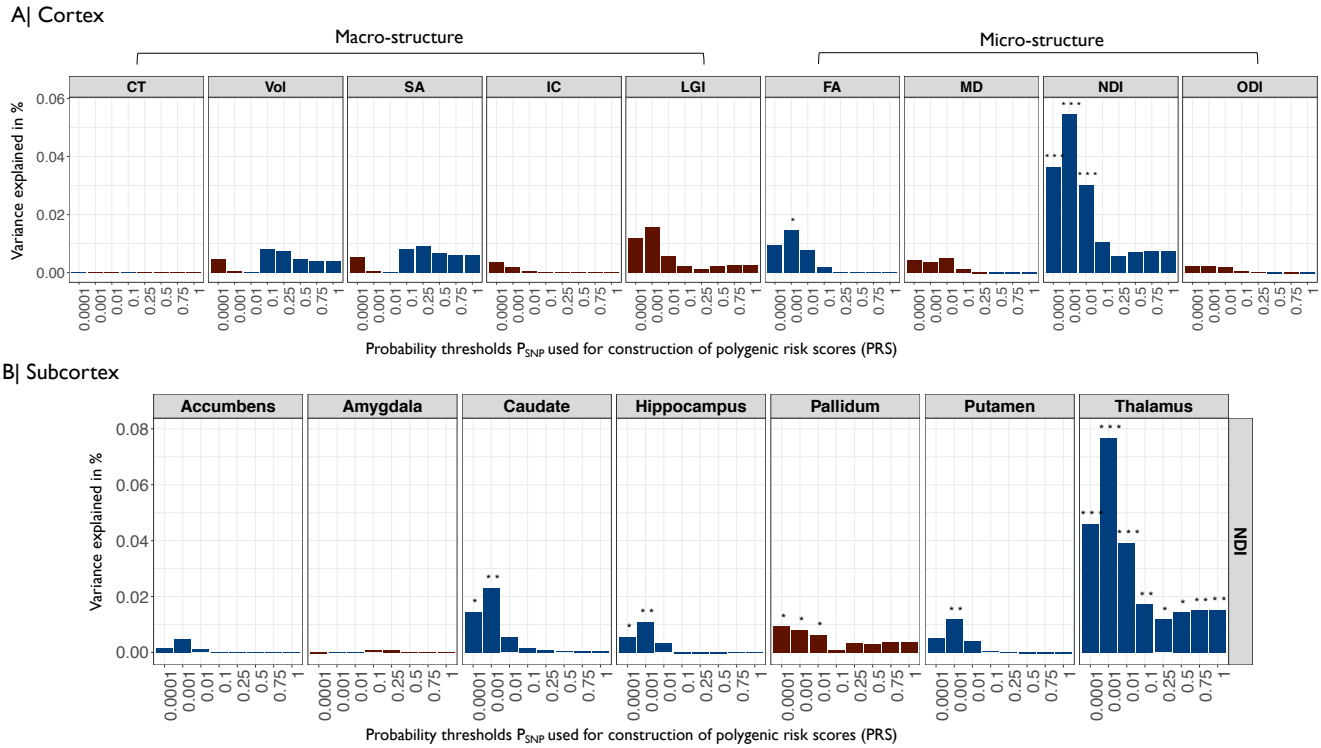

Figure 2. Associations between polygenic risk scores for schizophrenia and global cortical (A) and regional subcortical (B) metrics of human brain structure. (A) Barcharts of variance explained by schizophrenia PRS (R^2, y-axis) constructed at each of eight probability thresholds ($0.0001 \geq P_{SNP} \leq 1$, x-axis) for each of nine global mean cortical metrics: CT, cortical thickness; GMV, grey matter volume; SA surface area; IC intrinsic curvature; LGI local gyrification index; FA fractional anisotropy; MD mean diffusivity; NDI neurite density index; ODI orientation dispersion index. Blue bars indicate negative associations and red bars positive associations; asterisks indicate P-values for association after FDR correction: ($* \; P \leq 0.05$, $* * \; P \leq 0.01$, $* * * \; P \leq 0.001$). Polygenic risk scores for schizophrenia were significantly negatively associated with global neurite density index and fractional anisotropy. (B) Barcharts of variance explained by PRS (R^2, y-axis) constructed at each of eight probability thresholds ($0.0001 \geq P_{SNP} \leq 1$, x-axis) for NDI measured at each of seven subcortical regions (colours and asterisks code sign and significance of association as in A). PRS was significantly negatively associated with NDI in thalamus, hippocampus, putamen and caudate; and significantly positively associated with NDI in pallidum.

Regional cortical MRI phenotypes

As expected, we found that some of the MRI phenotypes were correlated with each other. The macro-structural markers of regional size (CT, SA, GMV) were positively correlated with each other and negatively correlated with LGI (a macro-structural marker of cortical surface gyrification). Among the micro-structural markers, NDI and FA were positively correlated with each other; and both were negatively correlated with MD and ODI (**Fig.3 A**).

We next tested the associations between MRI metrics at each of 180 cortical regions and the PRS constructed at the P_{SNP}-value accounting for the largest proportion of global variance of each MRI metric. There were significant associations between PRS and eight out of nine metrics in at least one cortical region, with the exception being CT (**Fig.3 B**). The proportion of regional variance explained by PRS ranged from $.002\% \leq R^2 \leq .08\%$ with $-.03 \leq \beta \leq +.03$; see **Table S7**.

Amongst the micro-structural markers, the highest number of regions significantly associated with PRS was found for NDI. Higher risk score was associated with significantly reduced NDI of 149 cortical areas (maximum R^2 = .06%, β = -0.03). The top ten regions where NDI was most strongly negatively associated with PRS were located in association auditory cortex, early auditory cortex, ventral visual stream, posterior cingulate cortex, insular and frontal opercular cortex, posterior opercular cortex, inferior parietal cortex and superior parietal cortex (see **Table S8** for details). FA was significantly negatively associated with PRS in 63 regions (maximum R^2 = .01%, β = -0.01); and positively associated with PRS in two regions (maximum R^2 = .01%, β = .01). The top ten regions where FA was most strongly associated with PRS were all areas of temporal, cingulate, frontal and insular cortex with decreased FA associated with higher risk scores. MD was significantly associated with PRS in 76 regions (66 positive and 10 negative associations). ODI was the micro-structural metric least frequently associated with PRS, at 11 cortical regions.

Of the macro-structural markers LGI showed the highest number of significant associations with PRS (72 regions; 67 positive and five negative) compared to GMV, SA and IC, each of which was significant in less than 15 regions (maximum $R^2 \leq .02\%$, maximum $|\beta| \leq .01$).

Since the MRI metrics were not independent of each other (**Fig.3 A**), we further explored the spatial co-localisation of genetic effects on different MRI metrics of regional cortical structure. The cortical t-maps of PRS association with NDI and FA were significantly positively correlated with each other, and were negatively correlated with the cortical t-maps of PRS associations with ODI (both NDI and FA) and MD (FA only) (**Fig.4 A**). In other words, regions where genetic risk was most strongly predictive of decreased FA ($\mathrm{FA}(t) \ll 0$) tended to be the same regions where PRS was most predictive of decreased NDI ($\mathrm{NDI}(t) \ll 0$) and most predictive of increased MD ($\mathrm{MD}(t) \gg 0$) (**Fig.4** B).

We also simply counted the number of different MRI phenotypes that were significantly associated with PRS at each of 180 cortical areas. There were genetic effects on at least two metrics in 122 regions (**Table S9**), at least three metrics in 68 regions and at least four metrics in 21 regions (**Fig.4** C). The most frequently co-localised genetic associations were with NDI and MD (63 regions) and NDI and FA (61 regions) (see **SI Results**). Regions that were associated with PRS in terms of multiple MRI phenotypes were located in (inferior) frontal, insular, temporal, auditory and ventral visual stream areas of cortex (**Fig.4 D , Table S9**).

Regional subcortical MRI phenotypes

We estimated the association between PRS and one macro-structural (GMV) and four micro-structural phenotypes (MD, FA, NDI, ODI) at seven subcortical regions. The single strongest effect was a negative association between PRS and NDI of thalamus ($R^2 = .08\%$, β -.03). NDI was also negatively associated with PRS in the caudate, hippocampus, and putamen; and positively associated with PRS in pallidum (**Fig.2 B**, **Table S10**). Further significant associations were found between PRS and MD of the amygdala, caudate, hippocampus, pallidum and putamen; between PRS and GMV of caudate, putamen and hippocampus; and between PRS and FA of putamen and thalamus; ODI of pallidum and thalamus **(SI Results)**.

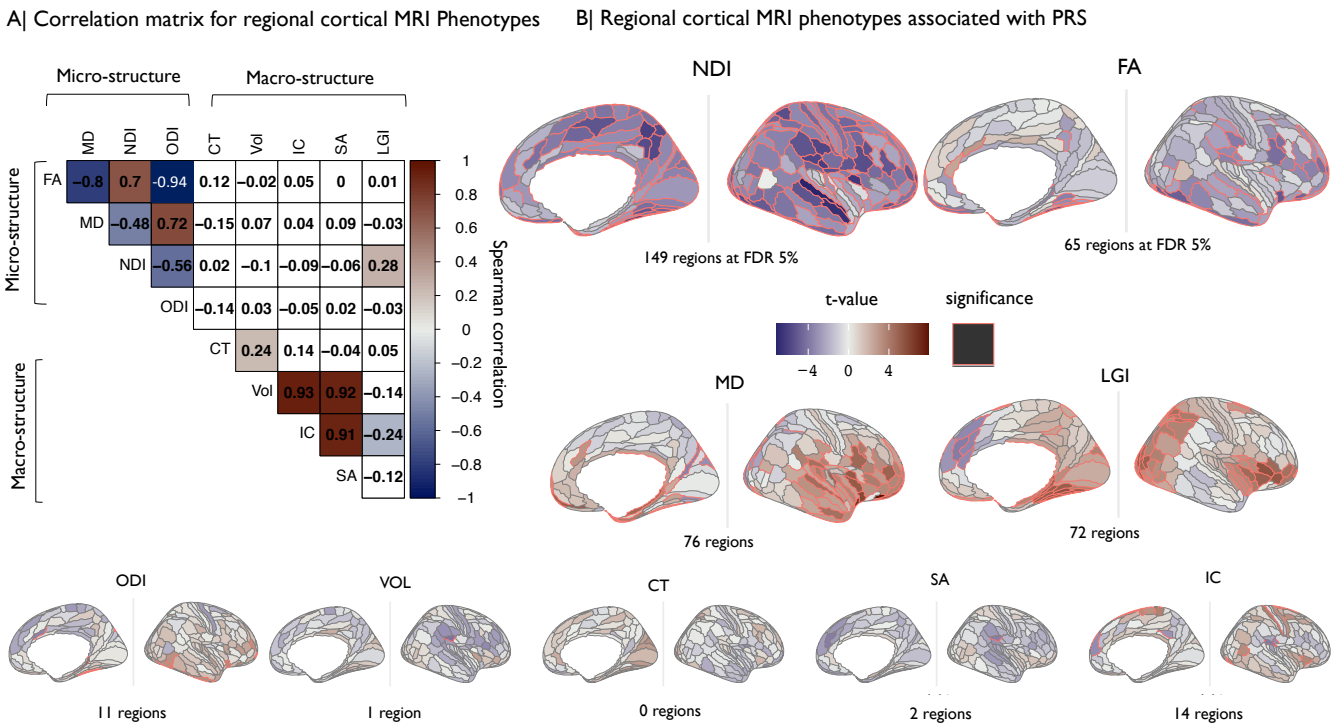

Figure 3. Regional cortical MRI phenotypes: correlations between metrics and associations of each metric with schizophrenia polygenic risk scores. (A) Matrix of Spearman's correlation for each pair of nine MRI metrics. Shades of blue indicate significant negative correlation and shades of red indicate significant positive correlations. (B) Cortical *t*-maps representing strength of association between schizophrenia PRS and regional MRI phenotypes; regions where the effect of PRS is statistically significant at FDR = 5% are outlined in red. NDI and FA metrics, which were globally decreased by genetic risk for schizophrenia (**Fig.2**), were significantly regionally decreased in multiple areas. MD and LGI metrics were significantly regionally increased by genetic risk in several areas.

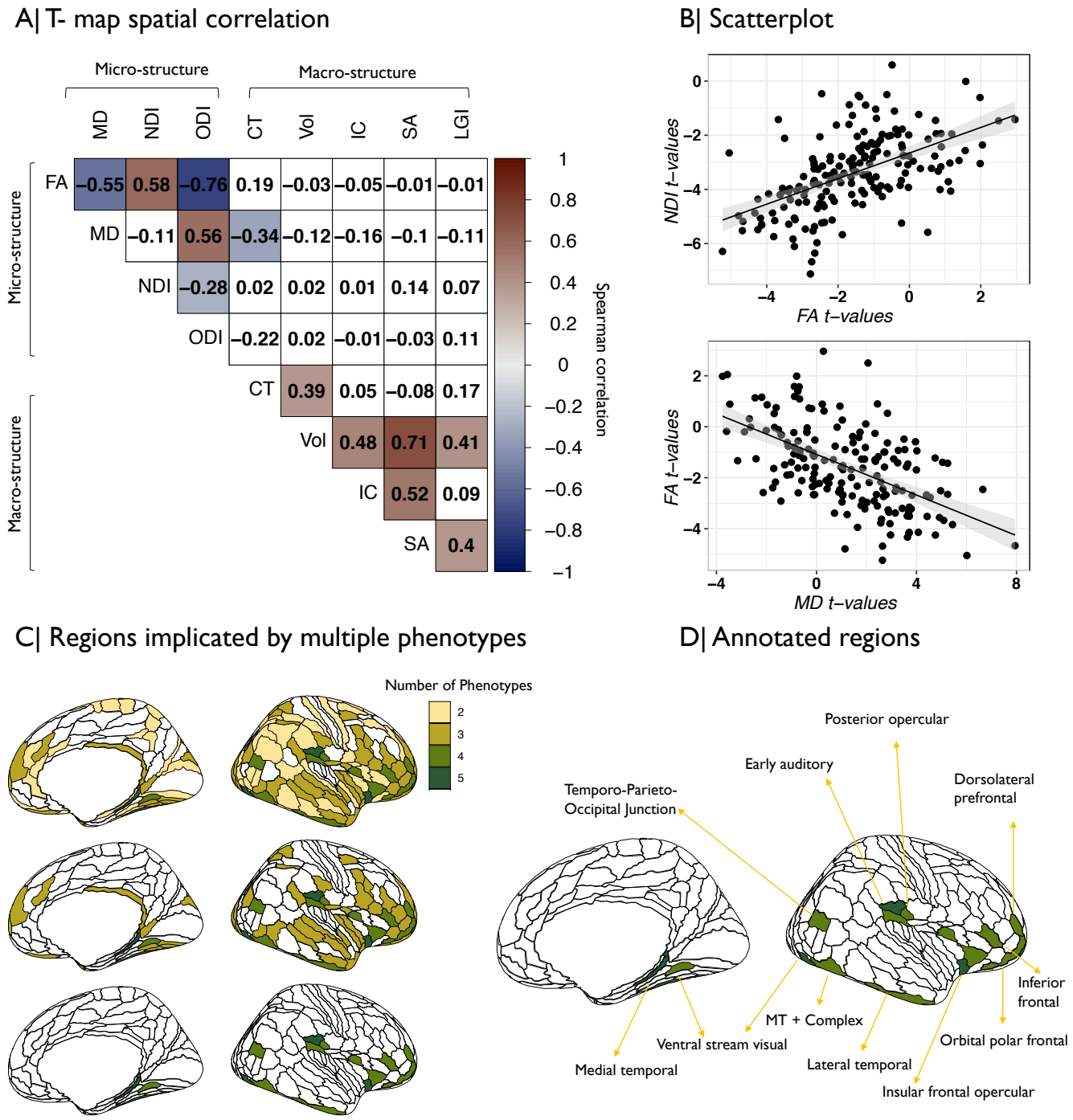

Figure 4. Anatomical co-localisation of polygenic risk effects for schizophrenia on multiple MRI phenotypes. (A) Matrix of spatial correlations between cortical *t*-maps of association between schizophrenia PRS and nine MRI metrics. (B) Scatterplot showing the relationships between (top) cortical *t*-maps of FA and NDI and (bottom) cortical *t*-maps of FA and MD; each point represents a cortical area. (C) Cortical map colour coded to indicate the number of MRI phenotypes that were significantly associated with schizophrenia PRS at each region. Coloured regions had at least two (top), three (middle), or four (bottom), MRI phenotypes significantly associated with genetic risk of schizophrenia. (D) The brain regions where schizophrenia PRS was significantly associated with four MRI phenotypes were anatomically located in medial and lateral temporal cortex, ventral visual stream, insular and frontal cortex.

Discussion

Structural brain abnormalities are thought to play an important role in the pathophysiological processes underlying schizophrenia and may be partially driven by genetic factors [46]. We estimated the effects of polygenic risk for schizophrenia on macro- and micro-structural MRI phenotypes measured at 180 cortical areas and seven subcortical structures. Using the largest imaging sample and the most powerful GWAS dataset published to date, we showed that PRS was significantly associated with micro-structural MRI metrics of tissue composition, at global and regional scales of cortex and in thalamus, basal ganglia and hippocampus. These results provide strong evidence in support of our hypothesis that polygenic risk for schizophrenia is associated with normative variation of neuronal tissue organization measurable by micro-structural MRI in the population.

Neurite density index - a plausible brain MRI marker for schizophrenia risk?

The investigation of multiple MRI phenotypes allowed us to compare their strength of association with polygenic risk for schizophrenia estimated in largely identical samples with consistent statistical methods. Of all nine MRI metrics considered, NDI was the most robustly associated with genetic risk: Higher polygenic risk for schizophrenia was negatively associated with NDI, explaining a greater proportion of variance in NDI than in any other metric. NDI is derived from NODDI, an MRI sequence that was developed to estimate the micro-structural complexity of dendrites and axons - collectively referred to as neurites - in the living brain. NODDI compartmentalizes tissue into three microstructural environments - intra-cellular, extra-cellular, and cerebro-spinal fluid - each of which shows different diffusion properties. The intra-cellular compartment refers to the space bound by neurites and allows for the measurement of their density (by the neurite density index) and their spatial orientation (by the orientation dispersion index) [47, 48]. *In vivo* estimates of NDI have been biologically validated by *ex vivo*, histological estimates of neuronal neurite density in mice [49]. In humans, NDI was strongly positively correlated with cortical myelination and negatively correlated with cortical thickness, suggesting that high NDI might be indicative of density of myelinated axons in the cortex [48].

Thus a reasonable interpretation of our results is that genetic risk factors for schizophrenia are associated with decreased axonal and dendritic density within cortical and subcortical grey matter structures. This interpretation is consistent with various lines of previous research linking NDI to schizophrenia. First, previous case-control imaging studies reported decreased NDI in schizophrenia cases with strongest effects in the temporal pole, hippocampus and parahippocampal gyrus [24]. Secondly, post-mortem case-control studies have reported multiple abnormalities of neurite structure in schizophrenia, including reduced dendritic arborisation in prefrontal and cingulate cortex [50], reduced spine density in prefrontal, visual, auditory cortex and the subiculum within the hippocampal formation [50], reduced axonal myelination [51], and a reduction of oligodendrocytes within grey matter [52]. Third, recent GWAS studies have identified risk genes for schizophrenia that are expressed in central nervous system neurons and implicated in dendritic microstructure and functional processes, such as synaptic organisation, differentiation and transmission [5, 53]. Fourth, locally reduced density of myelinated axons and dendrites will likely reflect reduced connectivity between brain structures, specifically cortico-cortical connections [51, 54], as anticipated by long-standing theories of schizophrenia as a dysconnectivity syndrome [55, 56, 57].

Integration of genetic effects across MRI phenotypes

While NDI was the most strongly associated with PRS, almost all other metrics (except CT) also showed some significant regional effects of genetic variation. We consider that this apparent pleiotropy of genetic effects on brain structure largely reflects correlations between the MRI metrics [58]. For example, NDI was positively correlated with FA, and both NDI and FA were negatively correlated with MD (**Fig. 3**). This occurs by construction because increased NDI restricts isotropic diffusion of protons in the tissue water compartment so that FA is increased and MD is decreased [58]. These three metrics are thus complementary measures of the same or similar tissue composition characteristics, which explains the anatomical co-localisation of genetic effects on NDI, FA and MD (**Fig. 4**). These co-localised, multi-metric effects of PRS were concentrated in auditory and lateral temporal cortex, pre-frontal and orbito-frontal cortex, anterior cingulate cortex, and insular cortical areas, many of which have previously been reported to show increased MD and/or decreased FA in case-control studies of schizophrenia [11, 21, 25, 26, 27, 28].

Of the macro-structural phenotypes, LGI was positively correlated with MD and positively associated with genetic risk for schizophrenia. LGI measures the amount of cortical folding and is assumed to capture early neurodevelopmental changes that are relatively stable after birth [23, 59]. Case-control data have recently shown increased cortical LGI in schizophrenia, which was interpreted as a marker of structural dysconnectivity [23]. Although genetic effects on LGI were partially overlapping with genetic effects on MD, e.g., in frontal cortex, the cortical t-map of schizophrenia PRS association with LGI was more strongly correlated with the cortical maps of genetic association with other macro-structural metrics (SA, GMV) than with the cortical t-map for MD or any of the other micro-structural metrics. Overall it is uncertain whether polygenic effects on LGI are mechanistically distinct from the co-localised genetic effects on correlated micro-structural markers of neurite density. However, it seems clear from these data that micro-structural MRI metrics are generally more sensitive to the effects of genetic risk for

schizophrenia compared to the macro-structural metrics that have previously been investigated as candidate endophenotypes.

The role of subcortical structures

Atypicality in subcortical structures is a frequently reported finding in schizophrenia cases [12], and in their non-psychotic first-degree relatives [60], compared to healthy controls. To the best of our knowledge, this is the first study to identify significant associations between polygenic risk for schizophrenia and subcortical structures in a population sample.

NDI was again the MRI metric most sensitive to genetic effects, especially in the thalamus, where PRS was significantly associated with reduced NDI. The thalamus is involved in the bidirectional exchange of neuronal signals between subcortical and cortical structures, as well as between cortical regions, and plays a key role in cognitive and emotional processes that are clinically impaired in schizophrenia [61, 62]. Structural and functional MRI case-control studies have previously reported volume reductions [61] and reduced prefrontal-thalamic and increased sensorimotor-thalamic connectivity in schizophrenia [63]. The basal ganglia (putamen, pallidum and caudate nucleus) and the hippocampus also demonstrated PRS-related changes in NDI and related micro-structural MRI metrics. There was also a robust (negative) association between PRS and volume of hippocampus, and reduced hippocampal volume is one of the most extensively replicated case-control differences reported in prior MRI studies of schizophrenia [12]. These subcortical effects of polygenic risk, especially in terms of reduced neurite density, are compatible with evidence that schizophrenia is associated with disruption of large-scale thalamo-striato-cortical circuits.

Strengths and limitations

It is a strength that we used the largest GWAS to date to construct schizophrenia PRS at multiple P_{SNP}-value thresholds for inclusion of risk variants. We also used the largest and most methodologically diverse MRI dataset to date in order to assess PRS associations with brain structure. However, the diagnostic variance in schizophrenia explained by PRS is still relatively small (7.7%) [5] and, in line with previous findings [16, 20], the proportion of variance in cortical and subcortical structures explained by the schizophrenia PRS is even smaller ($< 1\%$). It is expected that even larger sample sizes will lead to more powerful genetic associations, which in turn might implicate other brain structures or MRI metrics than those significantly associated with PRS in this study [5]. We have argued that the pattern of MRI results is plausibly attributable to genetic effects on specific aspects of cortical cytoarchitectonics (dendritic arborization) and myeloarchitectonics (myelinated axons). However, these interpretations could be more robustly supported by future translational MRI and histological studies of cortical micro-structure in human post mortem data or animal models of genetic risk for schizophrenia. The UK Biobank is an ageing cohort of largely European descent that is on average wealthier and healthier than the general population [64]. Comparable associations between PRS and MRI metrics of brain structure need to be investigated in more demographically diverse and epidemiologically relevant populations.

Summary

Polygenic risk scores for schizophrenia were most robustly associated with significant changes in cortical and subcortical micro-structural MRI metrics in a large population sample. These results provide substantial new evidence in support of the pathogenic model that genetic risk for schizophrenia is mediated by proximal effects on reduced neurite density, and therefore anatomical dysconnectivity, in specific cortico-subcortical networks.

Acknowledgements

E.-M.S is supported by a PhD studentship awarded by the Friends of Peterhouse. This research was co-funded by the National Institute of Health Research (NIHR) Cambridge Biomedical Research Centre and a Marmaduke Sheild grant to R.A.I.B. and V.W. E.T.B is an NIHR Senior Investigator. R.R.G was funded by a Guarantors of Brain Fellowship. R.A.I.B is supported by a British Academy Post-Doctoral fellowship and the Autism Research Trust. We wish to thank Dr Petra Vertes and Dr Lisa Ronan for their advice on research design and Dr Simon R White for his statistical advice and support. The views expressed are those of the author(s) and not necessarily those of the NHS, the NIHR or the Department of Health and Social Care.

Author contributions statement

E.-M.S., R.A.I.B., V.W., G.K.M. and E.T.B. designed research. J.S. advised on research design. E.-M.S., R.A.I.B., V.W., and R.R.G. analyzed data. E.-M.S. and R.A.I.B. made figures. E.-M.S., R.A.I.B. and V.W. performed research. E.-M.S. and E.T.B. wrote the paper.

Disclosures/Competing Interests statement

E.T.B. serves on the Scientific Advisory Board of Sosei Heptares and as a consultant for GlaxoSmithKline. All other authors declare no conflicts of interest.

References

1. Saha, S., Chant, D., Welham, J. & McGrath, J. A systematic review of the prevalence of schizophrenia. *PLoS Med* **2**, e141 (2005).

2. Pardiñas, A. F. *et al.* Common schizophrenia alleles are enriched in mutation-intolerant genes and in regions under strong background selection. *Nat. genetics* **50**, 381–389 (2018).

3. Hilker, R. *et al.* Heritability of schizophrenia and schizophrenia spectrum based on the nationwide danish twin register. *Biol. psychiatry* **83**, 492–498 (2018).

4. Sullivan, P. F., Kendler, K. S. & Neale, M. C. Schizophrenia as a complex trait: evidence from a meta-analysis of twin studies. *Arch. general psychiatry* **60**, 1187–1192 (2003).

5. Ripke, S., Walters, J. T., O'Donovan, M. C., of the Psychiatric Genomics Consortium, S. W. G. *et al.* Mapping genomic loci prioritises genes and implicates synaptic biology in schizophrenia. *medRxiv* (2020).

6. Riglin, L. *et al.* Schizophrenia risk alleles and neurodevelopmental outcomes in childhood: a population-based cohort study. *The Lancet Psychiatry* **4**, 57–62 (2017).

7. Gottesman, I. I. & Gould, T. D. The endophenotype concept in psychiatry: etymology and strategic intentions. *Am. journal psychiatry* **160**, 636–645 (2003).

8. Fornito, A. & Bullmore, E. T. Connectomic intermediate phenotypes for psychiatric disorders. *Front. psychiatry* **3**, 32 (2012).

9. Bigos, K. L. & Weinberger, D. R. Imaging genetics—days of future past. *Neuroimage* **53**, 804–809 (2010).

10. Bogdan, R. *et al.* Imaging genetics and genomics in psychiatry: a critical review of progress and potential. *Biol. psychiatry* **82**, 165–175 (2017).

11. Van Erp, T. G. *et al.* Cortical brain abnormalities in 4474 individuals with schizophrenia and 5098 control subjects via the enhancing neuro imaging genetics through meta analysis (enigma) consortium. *Biol. psychiatry* **84**, 644–654 (2018).

12. van Erp, T. G. *et al.* Subcortical brain volume abnormalities in 2028 individuals with schizophrenia and 2540 healthy controls via the enigma consortium. *Mol. psychiatry* **21**, 547–553 (2016).

13. Satizabal, C. L. *et al.* Genetic architecture of subcortical brain structures in 38,851 individuals. *Nat. genetics* **51**, 1624–1636 (2019).

14. Grasby, K. L. *et al.* The genetic architecture of the human cerebral cortex. *Science* **367** (2020).

15. van der Merwe, C. *et al.* Polygenic risk for schizophrenia and associated brain structural changes: A systematic review. *Compr. psychiatry* **88**, 77–82 (2019).

16. Reus, L. M. *et al.* Association of polygenic risk for major psychiatric illness with subcortical volumes and white matter integrity in uk biobank. *Sci. reports* **7**, 42140 (2017).

17. Franke, B. *et al.* Genetic influences on schizophrenia and subcortical brain volumes: large-scale proof of concept. *Nat. neuroscience* **19**, 420–431 (2016).

18. Grama, S. *et al.* Polygenic risk for schizophrenia and subcortical brain anatomy in the uk biobank cohort. *Transl. psychiatry* **10**, 1–10 (2020).

19. Van Scheltinga, A. F. T. *et al.* Genetic schizophrenia risk variants jointly modulate total brain and white matter volume. *Biol. psychiatry* **73**, 525–531 (2013).

20. Neilson, E. *et al.* Impact of polygenic risk for schizophrenia on cortical structure in uk biobank. *Biol. psychiatry* **86**, 536–544 (2019).

21. Ellison-Wright, I. & Bullmore, E. Anatomy of bipolar disorder and schizophrenia: a meta-analysis. *Schizophr. research* **117**, 1–12 (2010).

22. Ronan, L. *et al.* Consistency and interpretation of changes in millimeter-scale cortical intrinsic curvature across three independent datasets in schizophrenia. *Neuroimage* **63**, 611–621 (2012).

23. Sasabayashi, D. *et al.* Increased brain gyrification in the schizophrenia spectrum. *Psychiatry Clin. Neurosci.* **74**, 70–76 (2020).

24. Nazeri, A. *et al.* Gray matter neuritic microstructure deficits in schizophrenia and bipolar disorder. *Biol. psychiatry* **82**, 726–736 (2017).

25. McKenna, F. F., Miles, L., Babb, J. S., Goff, D. C. & Lazar, M. Diffusion kurtosis imaging of gray matter in schizophrenia. *Cortex* **121**, 201–224 (2019).

26. Narr, K. L. *et al.* Mean diffusivity: a biomarker for csf-related disease and genetic liability effects in schizophrenia. *Psychiatry Res. Neuroimaging* **171**, 20–32 (2009).

27. Spoletini, I. *et al.* Hippocampi, thalami, and accumbens microstructural damage in schizophrenia: a volumetry, diffusivity, and neuropsychological study. *Schizophr. bulletin* **37**, 118–130 (2011).

28. Kalus, P. *et al.* New evidence for involvement of the entorhinal region in schizophrenia: a combined mri volumetric and dti study. *Neuroimage* **24**, 1122–1129 (2005).

29. Woodward, N. & Parvatheni, P. M82. neurite orientation dispersion and density imaging (noddi) of the prefrontal cortex in psychosis. *Schizophr. Bull.* **43**, S240 (2017).

30. Choi, S. W. & O'Reilly, P. F. Prsice-2: Polygenic risk score software for biobank-scale data. *Gigascience* **8**, giz082 (2019).

31. Sudlow, C. *et al.* Uk biobank: an open access resource for identifying the causes of a wide range of complex diseases of middle and old age. *PLoS medicine* **12** (2015).

32. Alfaro-Almagro, F. *et al.* Image processing and quality control for the first 10,000 brain imaging datasets from uk biobank. *Neuroimage* **166**, 400–424 (2018).

33. Fischl, B. *et al.* Automatically Parcellating the Human Cerebral Cortex. *Cereb. Cortex* **14**, 11–22, DOI: 10.1093/cercor/bhg087 (2004). https://academic.oup.com/cercor/article-pdf/14/1/11/1193353/bhg087.pdf.

34. Glasser, M. F. *et al.* A multi-modal parcellation of human cerebral cortex. *Nature* **536**, 171–178 (2016).

35. Daducci, A. *et al.* Accelerated microstructure imaging via convex optimization (amico) from diffusion mri data. *NeuroImage* **105**, 32–44 (2015).

36. Bycroft, C. *et al.* The uk biobank resource with deep phenotyping and genomic data. *Nature* **562**, 203–209 (2018).

37. Yang, J., Lee, S. H., Goddard, M. E. & Visscher, P. M. Gcta: a tool for genome-wide complex trait analysis. *The Am. J. Hum. Genet.* **88**, 76–82 (2011).

38. Martin, A. R., Daly, M. J., Robinson, E. B., Hyman, S. E. & Neale, B. M. Predicting polygenic risk of psychiatric disorders. *Biol. psychiatry* **86**, 97–109 (2019).

39. Warrier, V. & Baron-Cohen, S. Childhood trauma, life-time self-harm, and suicidal behaviour and ideation are associated with polygenic scores for autism. *Mol. psychiatry* 1–15 (2019).

40. Privé, F., Vilhjálmsson, B. J., Aschard, H. & Blum, M. G. Making the most of clumping and thresholding for polygenic scores. *The Am. J. Hum. Genet.* **105**, 1213–1221 (2019).

41. Shen, X. *et al.* A phenome-wide association and mendelian randomisation study of polygenic risk for depression in uk biobank. *Nat. communications* **11**, 1–16 (2020).

42. R Core Team. *R: A Language and Environment for Statistical Computing*. R Foundation for Statistical Computing, Vienna, Austria (2018).

43. Smith, S. M. & Nichols, T. E. Statistical challenges in "big data" human neuroimaging. *Neuron* **97**, 263–268 (2018).

44. Shen, X. *et al.* Subcortical volume and white matter integrity abnormalities in major depressive disorder: findings from uk biobank imaging data. *Sci. reports* **7**, 1–10 (2017).

45. Yekutieli, D. & Benjamini, Y. Resampling-based false discovery rate controlling multiple test procedures for correlated test statistics. *J. Stat. Plan. Inference* **82**, 171–196 (1999).

46. Smeland, O. B., Frei, O., Dale, A. M. & Andreassen, O. A. The polygenic architecture of schizophrenia—rethinking pathogenesis and nosology. *Nat. Rev. Neurol.* 1–14 (2020).

47. Zhang, H., Schneider, T., Wheeler-Kingshott, C. A. & Alexander, D. C. Noddi: practical in vivo neurite orientation dispersion and density imaging of the human brain. *Neuroimage* **61**, 1000–1016 (2012).

48. Fukutomi, H. *et al.* Neurite imaging reveals microstructural variations in human cerebral cortical gray matter. *Neuroimage* **182**, 488–499 (2018).

49. Gong, N.-J., Dibb, R., Pletnikov, M., Benner, E. & Liu, C. Imaging microstructure with diffusion and susceptibility mr: neuronal density correlation in disrupted-in-schizophrenia-1 mutant mice. *NMR biomedicine* **33**, e4365 (2020).

50. Moyer, C. E., Shelton, M. A. & Sweet, R. A. Dendritic spine alterations in schizophrenia. *Neurosci. letters* **601**, 46–53 (2015).

51. Flynn, S. *et al.* Abnormalities of myelination in schizophrenia detected in vivo with mri, and post-mortem with analysis of oligodendrocyte proteins. *Mol. psychiatry* **8**, 811–820 (2003).

52. Raabe, F. J. *et al.* Oligodendrocytes as a new therapeutic target in schizophrenia: from histopathological findings to neuron-oligodendrocyte interaction. *Cells* **8**, 1496 (2019).

53. Sekar, A. *et al.* Schizophrenia risk from complex variation of complement component 4. *Nature* **530**, 177–183 (2016).

54. Alexander-Bloch, A. F. *et al.* Abnormal cortical growth in schizophrenia targets normative modules of synchronized development. *Biol. psychiatry* **76**, 438–446 (2014).

55. Schmitt, A., Hasan, A., Gruber, O. & Falkai, P. Schizophrenia as a disorder of disconnectivity. *Eur. archives psychiatry clinical neuroscience* **261**, 150 (2011).

56. Morgan, S. E. *et al.* Cortical patterning of abnormal morphometric similarity in psychosis is associated with brain expression of schizophrenia-related genes. *Proc. Natl. Acad. Sci.* **116**, 9604–9609 (2019).

57. Nelson, B. G., Bassett, D. S., Camchong, J., Bullmore, E. T. & Lim, K. O. Comparison of large-scale human brain functional and anatomical networks in schizophrenia. *NeuroImage: Clin.* **15**, 439–448 (2017).

58. Fukutomi, H. *et al.* Diffusion tensor model links to neurite orientation dispersion and density imaging at high b-value in cerebral cortical gray matter. *Sci. reports* **9**, 1–12 (2019).

59. Zilles, K., Palomero-Gallagher, N. & Amunts, K. Development of cortical folding during evolution and ontogeny. *Trends neurosciences* **36**, 275–284 (2013).

60. McIntosh, A. M. *et al.* Voxel-based morphometry of patients with schizophrenia or bipolar disorder and their unaffected relatives. *Biol. psychiatry* **56**, 544–552 (2004).

61. Pergola, G., Selvaggi, P., Trizio, S., Bertolino, A. & Blasi, G. The role of the thalamus in schizophrenia from a neuroimaging perspective. *Neurosci. & Biobehav. Rev.* **54**, 57–75 (2015).

62. Wagner, G. *et al.* Structural basis of the fronto-thalamic dysconnectivity in schizophrenia: a combined dcm-vbm study. *NeuroImage: Clin.* **3**, 95–105 (2013).

63. Chen, P., Ye, E., Jin, X., Zhu, Y. & Wang, L. Association between thalamocortical functional connectivity abnormalities and cognitive deficits in schizophrenia. *Sci. reports* **9**, 1–10 (2019).

64. Fry, A. *et al.* Comparison of sociodemographic and health-related characteristics of uk biobank participants with those of the general population. *Am. journal epidemiology* **186**, 1026–1034 (2017).

main